FOURIER TRANSFORM SPECTROSCOPY

A Major Qualifying Project

Submitted to the Faculty of

Worcester Polytechnic Institute

in partial fulfillment of the requirements for the

Degree in Bachelor of Science

in

Physics

By

Darien Gaudet

Hayden Savage

Date: 4/24/19

Project Advisor:

Professor Richard Quimby

This report represents work of WPI undergraduate students submitted to the faculty as evidence of a degree requirement. WPI routinely publishes these reports on its web site without editorial or peer review. For more information about the projects program at WPI, see http://www.wpi.edu/Academics/Projects.

Abstract

Today, Fourier transform spectroscopy has cemented itself as a widespread method of spectral collection and analysis. However, comprehending the fundamentals of the technique is often a daunting challenge. To provide a simple and efficient means of learning FTS, we set out to create a student module founded on first-hand experimentalism. Various light sources were implemented to generate data for our mathematical computations. Thorough testing revealed that some of the equipment we used was defective, preventing implementation of the Fourier transform. As a result of this, the goal was refocused more on teaching students the fundamental principles of interferometry without the focus on the Fourier transform method.

Acknowledgements

We would like to thank our adviser, Dr. Richard Quimby, for serving as a highly knowledgeable, and incredibly insightful resource.

Contents

1. Introduction

1.1 Project Goals

This study explores and refines the necessary techniques of Fourier transform spectroscopy and interferometry, and packages the essential components in a form which serves undergraduates. An essential basis for this project was the TeachSpin reference sheets, which allowed us to achieve accelerated insight into the experimental materials. Our methodology is at its conclusion an executable module for learning, and a guide for condensing complicated learning materials into accessible instruction towards proficiency with these concepts. This project differentiates itself from works of similar strains by our focus towards Fourier analysis and signal processing, which stretches beyond optical testing. Our module is optimized such that it is consistent with verifiable lab data, and also consistent with the academic requirements imposed by Worcester Polytechnic Institute. We seek to promote the optimal conditions for hands-on learning environments, namely those where students freely manipulate configurations themselves. We wish to acquaint students with interferometric techniques, basic spectral analysis, and practice with optics more generally. Our module prioritizes experimentation, and readily compliments conventional learning materials. The completion of the module provides a wide and realistic foundation for students interested in spectroscopy. It could be said that our objectives are in close association with those of WPI, particularly, "Theory and Practice."

1.2 Literature Review

Fairly shortly into our reading, we discovered that numerous universities had undertook similar efforts to construct their own related lab modules. At first, we noticed lab sheets which promised similar goals to those of our own. For example, we identified an interesting and characteristic lab sheet from Fullerton College. The Fullerton lab module created an ever-broadening scope of experiments which began with exercises on two-source interference and standing waves, and it used fairly simplistic materials such as weights and pulleys. These materials caught our interest because often the most simplistic materials provide the best visualization of a concept. This also suggests that the module was intended for a less specialized audience, and likely meant to span over a wide time period because of its rudimentary starting point and extensive coverage. Due to the fact that we confined our module length to seven weeks, in accordance with a quarter system, examining the Fullerton module and condensing its principles became a microcosm of our project entirely. Next, their experiment module digressed into wave optics, where students measured the diameter of a human hair by using its thin width to generate a diffraction pattern. The lab portion of the module also made students familiar with a Helium-Neon (HeNe) laser and basic double slit experiments. The next part offered the chance to familiarize students with the Michelson interferometer, just as we make use of in this project. To summarize the specialty of the Michelson configuration, they discuss its “classical” functionality; measuring finite changes in index of refraction, comparing atomic standards to one another, ect. The lab module also examines the Michelson interferometer’s capability to facilitate white light sources with an equal-arm condition to measure unknown indexes of refraction. They also discuss the spacing measurement of a sodium

doublet, a concept we utilize within the course of our study. The final, interesting component of this extended module was a reference sheet detailing proper statistical analysis and error formality. This too is a concept we emphasize to anyone practicing proficient science.

2. Theory

Spectroscopy is the study of the interaction between light and matter. When we refer to a spectrum, we refer to a plot of light intensity against some wavenumber (reciprocal wavelength). Fourier transform spectroscopy is a unique form which uses the relative phase of waves to produce spectra. It is particularly useful in determining substance composition, and works well in the infrared light spectrum. One of the main advantages of Fourier transform spectroscopy is a greater signal-to-noise ratio, which is a result of higher throughput power to the detector. Spectral procurement also occurs on a much shorter timescale than traditional methods. In this section we will demonstrate the basic concepts of spectroscopy and interferometry, and refer with high priority to the Fourier transform technique. This section will outline the key concepts needed to understand the methodology of our experimental practice. This means that we cannot realistically cover the advanced mathematics of many of these concepts, but will instead trace the parts essential for understanding our work.

2.1 Interferometry

An interferometer is an apparatus which allows simple measurement of a multitude of quantities. Some of the most prominent of these are material analysis, surface and thickness analysis, distance measurement, optical power measurement, measurement of electric and magnetic fields, and even the detection of gravitational waves. To conduct Fourier transform spectroscopy for optical testing such as our own, it is most suitable to use an interferometer. For our purposes, we sought to collect information about the relative phase of two-beams, as a function of optical path difference (OPD), the spatial difference of light traveled in two optical fields. This goal renders the use of a Michelson interferometer quite appealing. Before we discuss the components of our specific bench configuration, we will discuss the concept of path difference, the defining characteristic of the interferometer.

2.1.1 Optical Path Difference

The OPD signifies a discrepancy of phase between the two beams, and multiple signal measurements at discrete points of difference generates an interferogram. Thus, the interferogram is record of the interference pattern. This concept is quite useful in terms of the Fourier transform. If two beams are from the same source, each with the same origin phase, we can define

$$OPD = \frac{\lambda}{2\pi}\Delta\Phi \tag{2.1}$$

where $\Delta\Phi = \Phi_1 - \Phi_2$ is the relative phase difference. However, this definition is less useful in a practical setting where we would not be calculating the OPD, but instead measuring it. Rearranging the above equation to solve for the relative phase difference is possible once the OPD becomes an experimental parameter. In an interferometer used for our purposes, spatial distance determines path length. Therefore, for a two beam configuration, the OPD is best understood as

$$OPD = p_1 - p_2 = n_1 d_1 - n_2 d_2 \tag{2.2}$$

where $p_i$represents a path, n_i a refractive index, and d_i the length of the path. In this case, index i is integer 1 or 2. In an example, where let's say we change p_1 by some distance δ, such that $p_1 = (d_1 + \delta)n_1$, and we count N oscillations, the wavelength $\lambda = 2\delta/N$. This will be important for when we use the OPD to calculate the source wavelength directly.

The OPD can also be written as a time delay

$$\tau = \frac{OPD}{c} = \frac{\lambda}{2\pi c}\Delta\Phi \tag{2.3}$$

where c is the speed of light in a vacuum. This is simply another way to conceptualize a non-zero OPD, whereby the spatial distance is conceived of as a time functional. Therefore, in the last analysis, the interferogram is conceptually equivalent to a continuous time signal. This concept proves quite convenient to our discussion of the interferogram and Fourier transform.

2.1.2 Wave Interference

Interferometric optics is founded on the study of wave interference, whereby two or more waves (for our purposes, light) combine to create a superposition of wave crest and trough. This leads to constructive or destructive interference, depending on which segment of the waves are "simultaneous" with each other. If the $OPD = 0$, i.e., the "equal-arm" condition, light will interfere constructively and the center of the interference "bullseye" will be illuminated. In the case of monochromatic light, such as that of lasers, two-beam interference can be expressed as

$$I(x,y) = I_1 + I_2 + 2\sqrt{I_1 I_2}\cos(\Phi_1 - \Phi_2) \tag{2.4}$$

Here, I represents the irradiance (intensity) of the beams and $\Phi_1 - \Phi_2$ the phase difference in radians. This means that intensity varies with cosinusoidal term, producing the alternating "dark" and "light" rings known as an interference pattern, where light bands represent constructive interference, and dark bands destructive. Because the energy of a wave is proportional to its squared amplitude (complex amplitudes), we can substitute amplitudes for I_1 and I_2. This gives us

$$I(x,y) = {A^2}_1 + {A^2}_2 + 2A_1 A_2\cos(\Phi_1 - \Phi_2) \tag{2.5}$$

Thus, the maxima occur when the phase difference is a multiple of 2π. This of course implies that both beams are of the same polarization. Beams of different polarization do not sum with each other, both constructively and destructively. We will further discuss some essential conditions for generating interference patterns in the next section.

2.1.3 Generating Interference Fringes

Let us pretend we are seeking to observe interference fringes of two beams on some area. To proceed, we must ensure certain conditions are met. Generally, the two beams must be coherent with each other (temporal and spatial) and have matching polarity. Furthermore, the irradiance of the beams must be similar in magnitude. These conditions will be easily met if, for example, a common source is used to generate the interfering light. Sources are capable of generating fringes so long as optical path

difference between them is smaller than its coherence length. Calculating the coherence length is rather simple

$$L_c = \frac{\lambda_m^2}{\Delta\lambda} \tag{2.6}$$

and from there, we calculate the coherence time

$$t_c = \frac{L_c}{c} \tag{2.7}$$

The middle, or center wavelength is given as λ_m, the spectral bandwidth is given as $\Delta\lambda$, and c is the speed of light in a vacuum.

2.1.4 Interferometric Visibility

Visibility, or for our purposes, Michelson visibility, is a measure of fringe contrast within a two-beam, linear interferometer system. Visibility depends on the optical path difference (OPD) between the beams, and is often written as $V(OPD)$. It can also be thought of as the degree of coherence between two optical fields. Visibility is a value between 0 and 1, respectively representing zero-visibility to maximum visibility. For practical purposes, $V(OPD) > 0.2$ will generally produce distinct fringes. Below is the modified two-beam interference equation.

$$I(x,y) = I_1 + I_2 + 2\sqrt{I_1 I_2}\cos(\Phi_1 - \Phi_2) * V(OPD) \tag{2.8}$$

Where $V = (I_{max} - I_{min})/(I_{max} + I_{min})$ in regards to maximum and minimum intensities.

For lasers, $V(OPD)$ approaches 1, and this modification is generally negligible. The maximum visibility occurs when the ratio of I_1/I_2 equals 1. In terms of our project, we largely worked with laser sources,

rendering visibility a non-factor. However, it became important once we made use of more recognizably extended sources.

2.1.5 The Michelson configuration

There are numerous methods of constructing an interferometer. It will suffice to note that some configurations are superior for certain measurements, and that configurations are largely dependent on observed variables. For the purpose of measuring spatial distances, or conducting optical testing, the Michelson interferometer is the most suitable.

Figure 2.1: Schematic diagram of our Michelson configuration

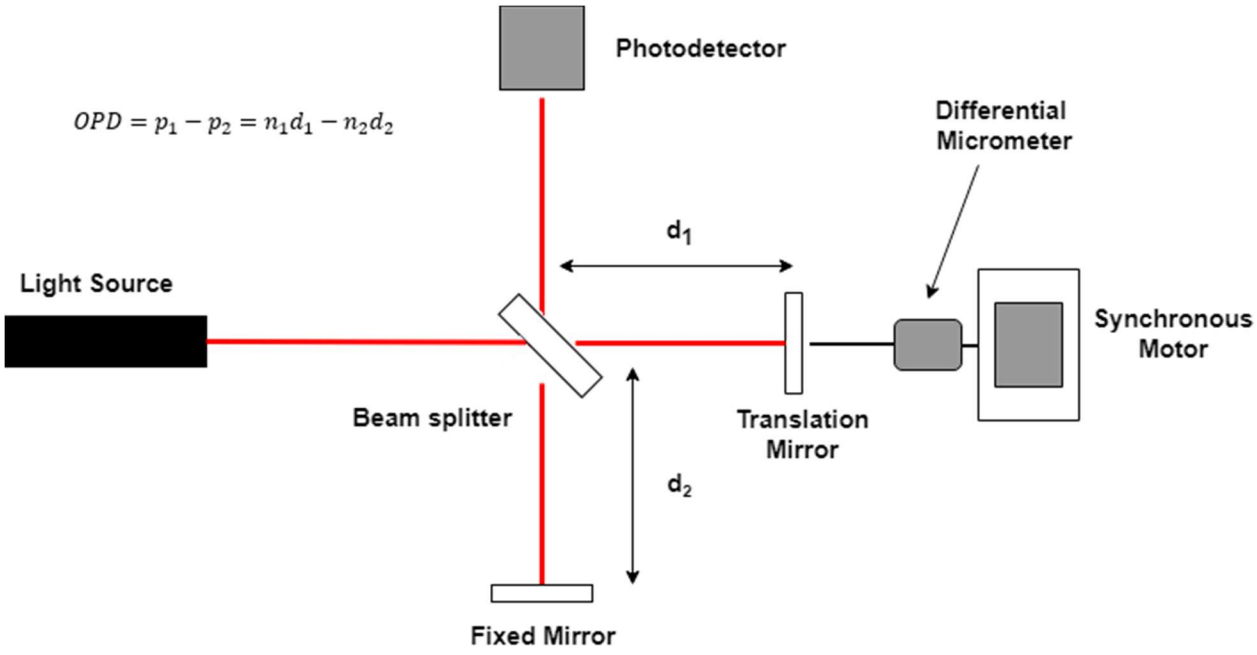

The Michelson interferometer has several distinguishing features. Primarily, amplitude division using a beam splitter, which transmits one beam and reflects the other across two orthogonal paths relative to the beam splitter. The whole wavefront is divided at the same point, and in theory, two beams of half intensity are produced. One mirror is fixed after being adjusted to meet the equal-arm condition. The equal-arm condition occurs when the OPD is zero, and is initially significant for producing an interferogram. The second mirror, a translation mirror, is consistently adjusted at a constant rate, and this translation creates a non-zero ODP, continuously altering the interference pattern. As shown in FIG2.1, we made use of a synchronous motor to drive a differential micrometer at a constant angular velocity. A differential micrometer is unique because it allows for extremely small, and fine-tuned alterations to be made, and is based upon the concept of a differential screw. This type of screw is known for its unique threads. As shown in the figure, the differential micrometer makes contact with a

pushrod axel, which is fed into the translation stage, driving the movement of the mobile mirror. After the beams reflect from the two mirrors, they recombine at the beam splitter and encounter a photodetector, which measures the time-signal (as a result of the time delay). Essentially, what has just occurred is the simultaneous measurement of all wavelengths of the source, and the conversion of the OPD to an electric time-signal.

Figure 2.2: Our Michelson configuration as operated on the bench.

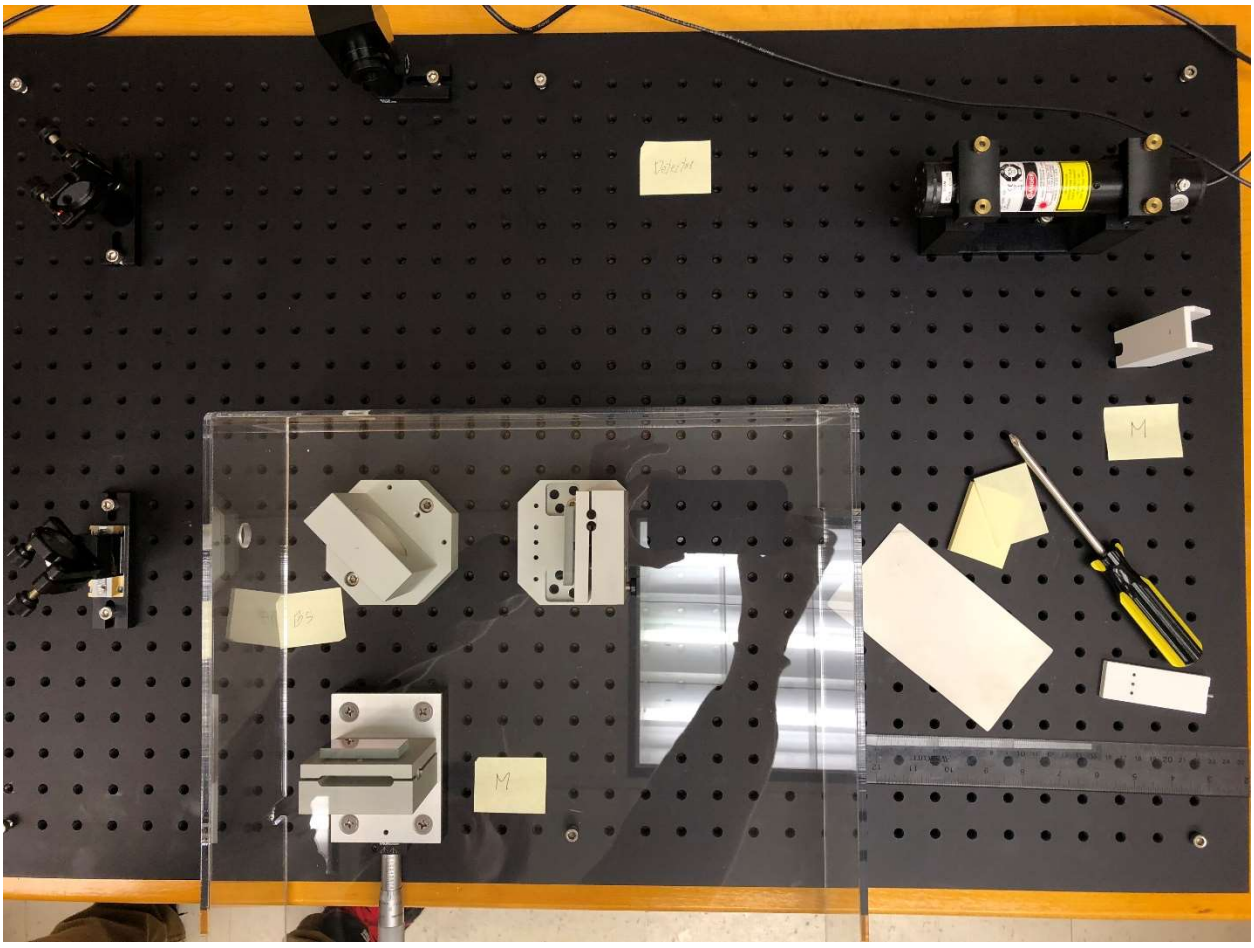

FIG2.2 is the actual configuration we used for our experimental data analysis, from a top-down bench view. Notice the area under the draft cap contains the essential components of the interferometer (Translation stage, mirrors, and beamsplitter). Also, notice the two elbow mirrors on the left-hand side of the figure, which are not listed in FIG2.1. These mirrors are suitable for a compact arrangement such

as our own, where the laser does not point directly at the beam splitter, and any adverse effects are negligible.

2.2 Signal Analysis

The electrical signal generated by the photodetector can be observed in real time using an oscilloscope, whereby one can monitor the signal-to-noise ratio. After some translation distance δ of the mobile mirror, the interferogram can be processed in a number of ways; the most significant of which is via a mathematical functional, the Fourier transform.

2.2.1 The Fourier Transform

Fourier transforms appear pervasively across a wide variety of scientific branches, beyond strictly mathematical disciplines. Therefore, while it may seem tempting to regard the Fourier transform as a mathematical functional in its entirety, such an assertion is shortsighted. The Fourier transform has very well defined physical representation. This is shown simply by the fact that a waveform (optical, acoustic, electrical) is the Fourier transform of its spectra, and vice versa. For the purposes of this project, we discuss the Fourier transform of the interferogram, which is the source light spectrum. The Fourier Transform could be understood as the extension of the period in the Fourier series to infinity, and its derivation comes from manipulation of the Fourier series synthesis equations. The Fourier Transform decomposes a time signal into all of the frequencies which constitute it. It can be thought of as straining out the individual components in a mixture, and each component can be measured in magnitude of "quantity." For our purposes, we are interested in the physical representation of the transform, particularly between the time and frequency domain. The resulting spectrum $S(f)$ of some electrical waveform $V(t)$ is the Fourier transform of that waveform. This can be represented as

$$S(f) = \int_{-\infty}^{\infty} V(t) e^{-i2\pi f t} dt \tag{2.9}$$

which indicates the cyclical property of the transform via its complex exponential. As alluded to earlier, the Fourier transform is a reversible functional, ie, the time domain signal $V(t)$ is also the Fourier transform of the spectrum $S(f)$. Generally, we call these transform pairs. The corresponding transform pair is written as

$$V(t) = \int_{-\infty}^{\infty} S(f) e^{i2\pi f t} df \tag{2.10}$$

Since $V(t)$ is restricted to real functions, by nature of physically possible time-dependence, $S(f)$ is Hermitian, and its real component must be even. In our project we made use a discrete form of Fourier transform called the Fast Fourier transform (FFT), which to put simply, factors the transform matrix, breaking down longer computations to combine. Signal processing constituted a majority of our data analysis, which we will discuss in greater detail in the next section.

3. Experiment and Results

3.1 Early Stages

At the beginning of the project, the equipment was not yet available for constructing the Michelson interferometer. Instead of physical experimentation, simulations were run using MATLAB to ensure that implementation of the Fourier transform was done correctly, as well as to predict limitations on factors such as scan length and spectral resolution.

The MATLAB simulation began with a pre-defined spectrum that was to be replicated as though obtained from an interferometer. The simulation took a mesh of points along the spectrum and generated pure sine waves with wavenumbers corresponding to each mesh point. Then at each of a series of simulated mirror path differences, the total intensity incident on the detector was calculated by taking the sum of all the sine waves for different wavenumbers. Once this was complete, an interferogram was generated using the simulated data for intensity vs. mirror path difference. The mirror path difference was measured in centimeters, and the units for intensity were arbitrary, since on the final spectrum in a real life scenario, all that matters are relative intensities of important features. This interferogram was representative of the real data that would later be gathered in the laboratory using the Michelson interferometer. Once the interferogram had been generated, the data were fed into MATLAB's built-in FFT (Fast Fourier Transform) function. This function returns complex values, so the absolute value of the output was taken to ensure that the intensity values in the final spectrum were real and positive.

In the first test, Gaussian curves were used as inputs, with progressively smaller bandwidths. The purpose of this test was to determine how bandwidth affected resolution of the FFT-obtained spectrum. Figure 3.1 contains graphs showing the results of a few of these.

Figure 3.1 - Simulated Bandwidth Variation

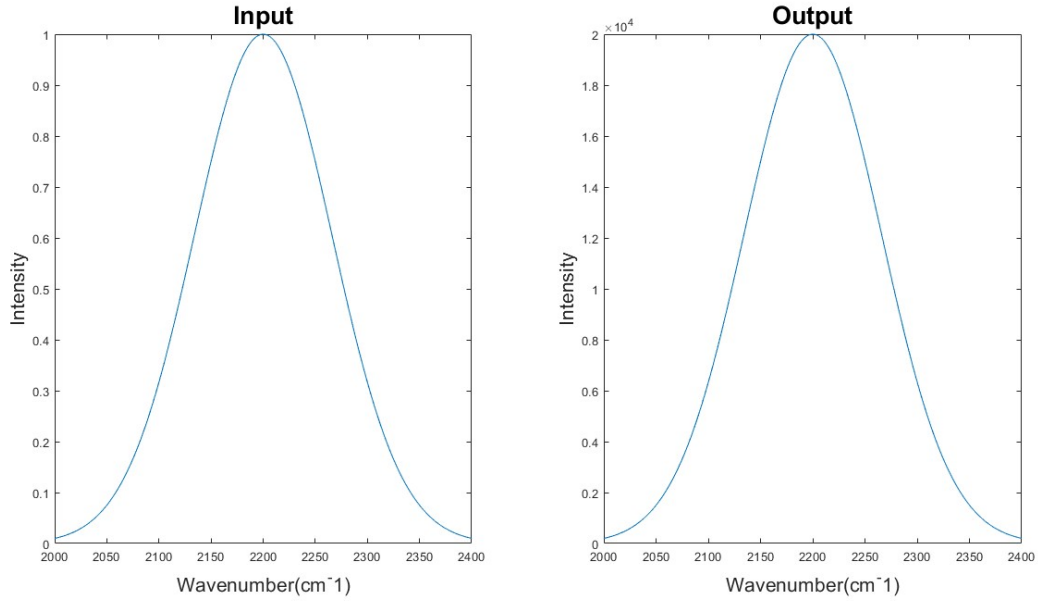

a) It is clear in this graph with a wide bandwidth that the input distribution has been recreated faithfully.

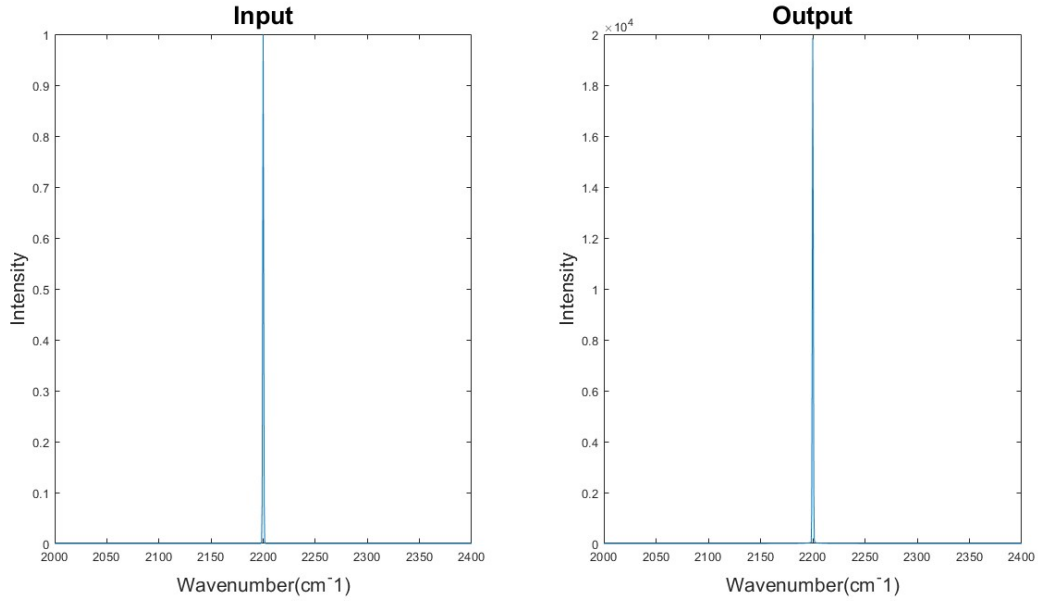

b) Here the bandwidth is very thin, but it is clear that the output is faithful, since it does not display the same abnormality present in c).

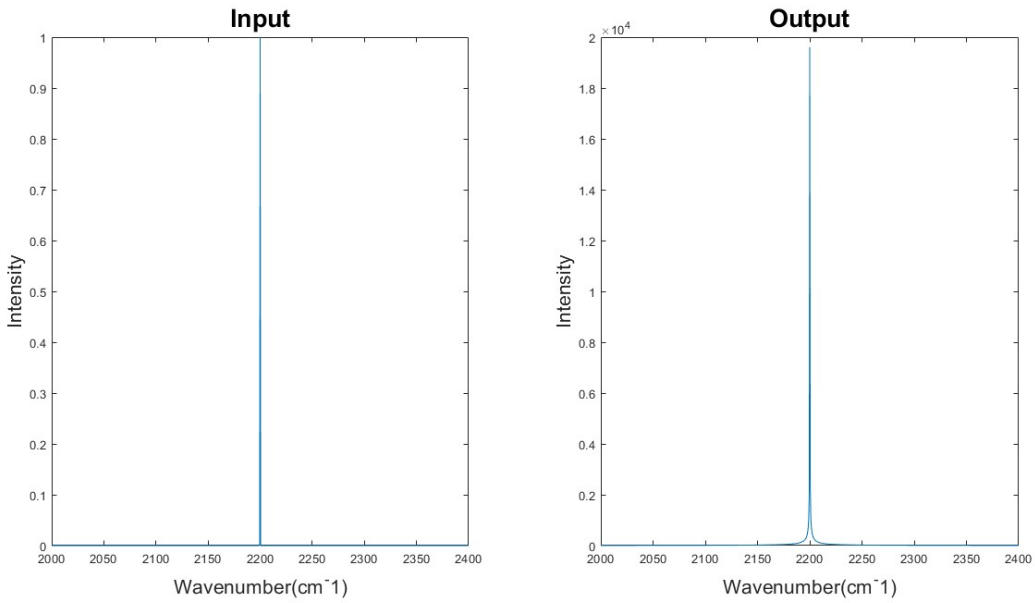

c) Here a noticeable flare is visible at the bottom of the output distribution that is not present in the input.

Fig. 3.1.a shows a simulation of a relatively broadband source, and is mainly useful for demonstrating that the simulation is functional. Fig 3.1.b shows a simulation with a source of a narrow but finite bandwidth. This demonstrates that even narrow band sources can be recreated effectively. Fig. 3.1.c shows a simulation in which the bandwidth of the Gaussian curve became so narrow that due to the finite resolution of the mesh on the input distribution, it was indistinguishable from a delta function. Clearly, the simulated spectrometer was unable to replicate this, as the output spectrum is visibly spread out across a range of wavenumbers.
This suggests that spectra obtained in this way will be faithful even for narrow band sources, provided that the bandwidth is sufficiently larger than the resolution. This was promising, since even lasers, which are designed to be narrowband sources, do have a wavelength spread, so an experimental setup with sufficient resolution should be able to accurately recreate the spectrum of a laser beam.

The next test used delta functions as input distributions, and varied the wavenumber to see if and how the amount of spread varied with different wavenumbers. Demonstrative graphs are shown in Figure 3.2.

Figure 3.2 - Simulated Wavenumber Variation

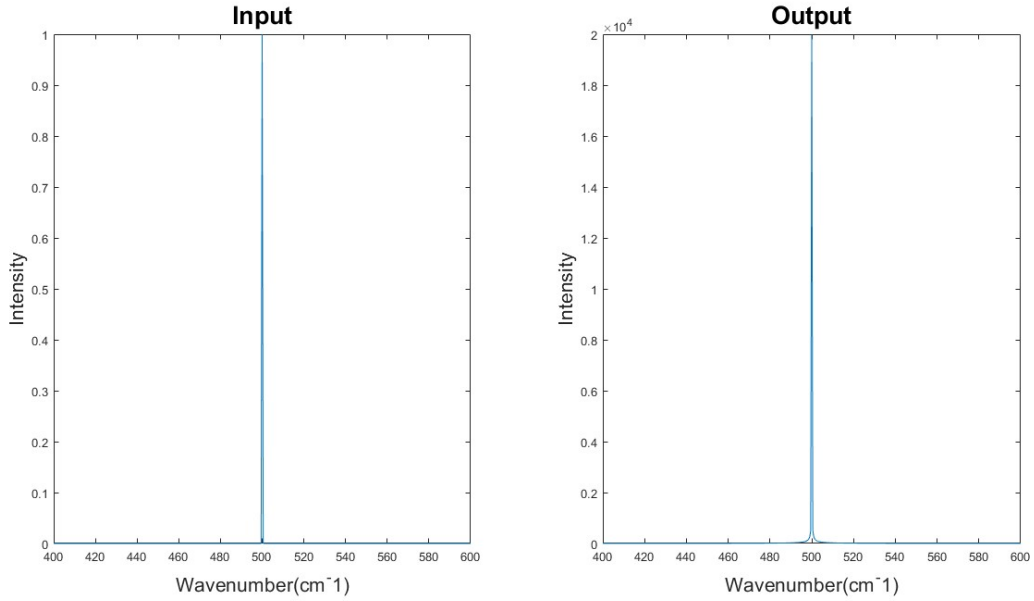

a) Here the wavenumber is low, and the spread is narrow.

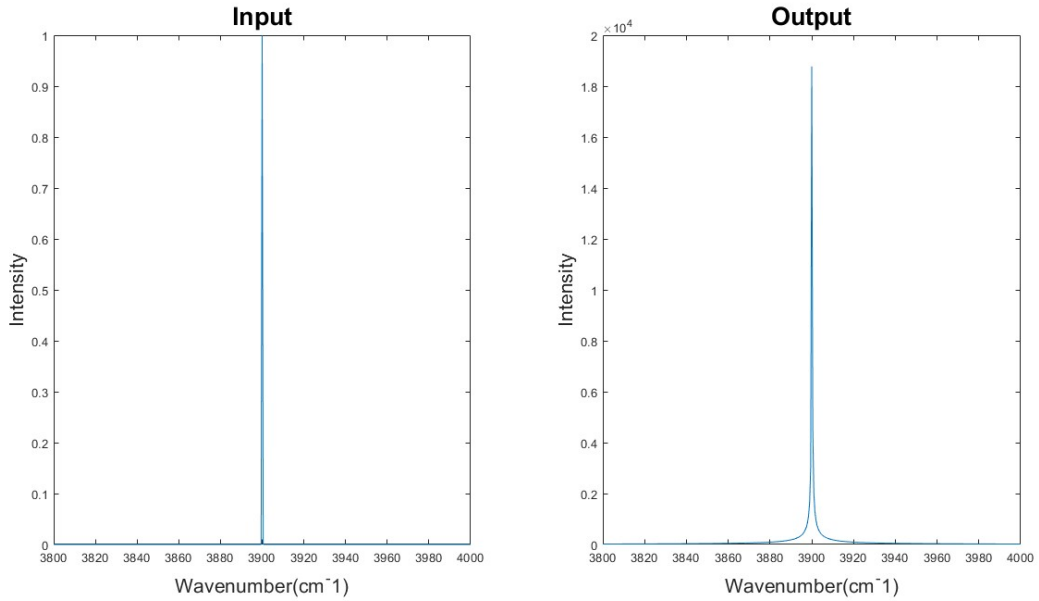

b) Here the wavenumber is high, and the spread is wide.

Fig. 3.2 only shows the extreme ends of the range tested, but this trend was visible throughout the test. The amount of spread added to the delta function during processing increases for increasing wavenumber (or decreasing wavelength). This means that in general, lower wavenumbers (higher wavelengths) will allow for better results.

The final test run using the simulation used a delta function once again, and the parameter that was varied was the distance that the movable mirror moved; the scan range. This test would reveal the relationship between the scan range and the spreading of the delta function. Figure 3.3 shows some of these results.

Figure 3.3 - Simulated Scan Range Variation

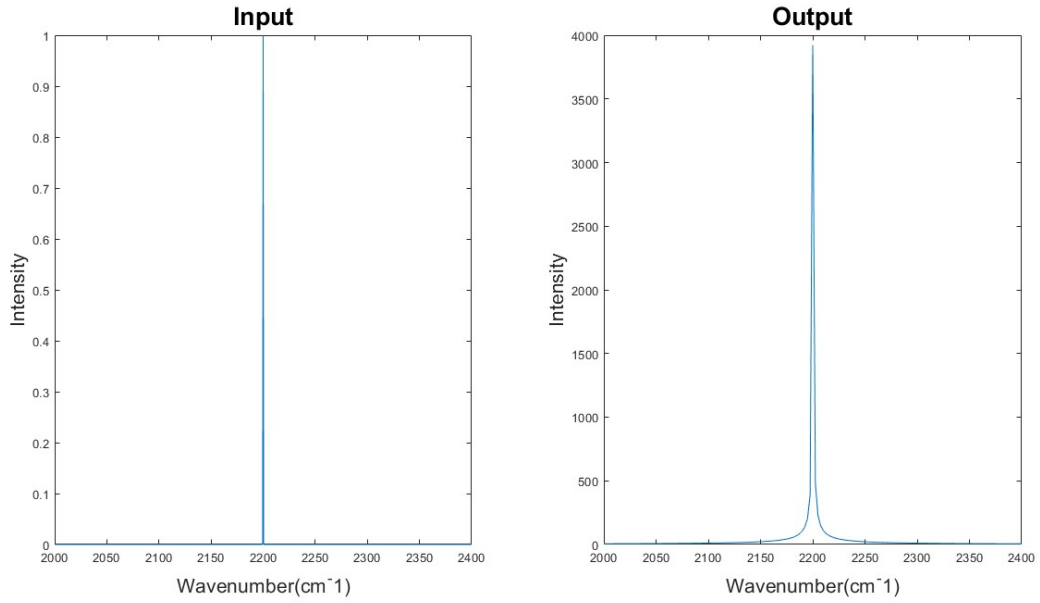

a) This scan used a relatively short scan range, and the spread of wavenumbers is quite wide.

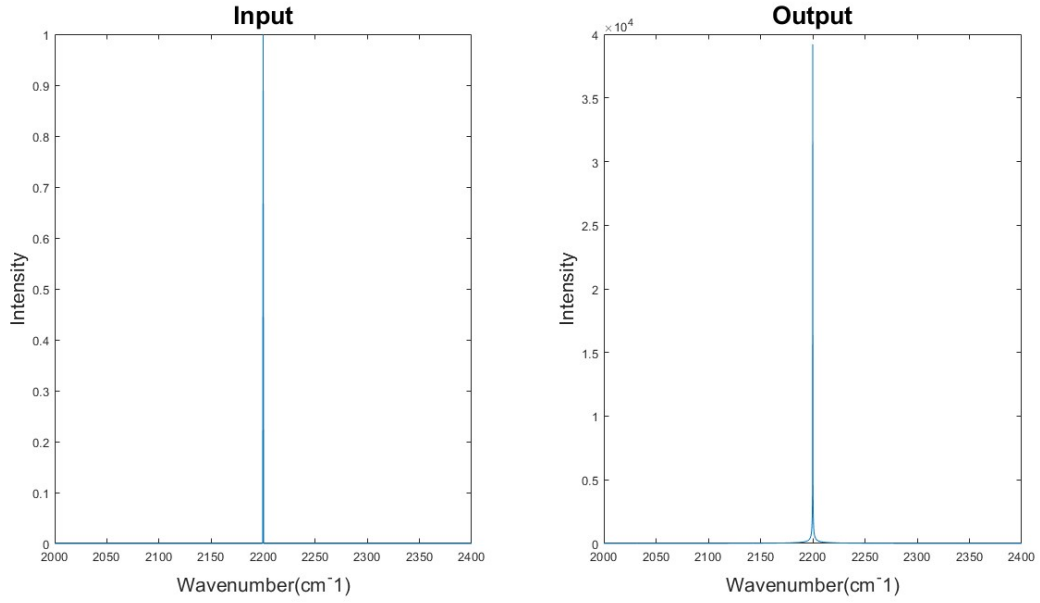

b) This scan used a relatively long scan range, and the spread is much smaller.

The spread is large for short scan ranges, and small for long scan ranges. This shows that for the sake of accuracy, longer scans are more desirable.

Once the tests had been conducted and the equipment had arrived, the Michelson interferometer was constructed. The process of aligning the various mirrors was time consuming, so for a several lab sessions no progress was made on experimentation. This experience was somewhat informative, however, as it made clear the fact that performing a full alignment from scratch would be unreasonable for the time constraints of an undergraduate lab module. This made it apparent that an

alternative would need to be devised. Once the interferometer was constructed and properly aligned, it was time to begin the experimental phase.

3.2 Main Experimental Phase

The data were gathered by a computer program, and analyzed using MATLAB. The experimental procedure for gathering data was as follows: A differential micrometer connected to the movable mirror in the Michelson interferometer would be set to a predetermined starting position, and the micrometer reading corresponding to this position would be recorded. A motor would be connected to the micrometer in order to rotate it smoothly. Early in the experimental phase, the motor and the data acquisition would be started at the same time. Later this part of the procedure was changed so that data acquisition would be started while the detector was covered, then the motor would be started with the micrometer preset to a bit before the starting position, allowing the motor to get up to speed, then once the micrometer reached the starting position, the detector was uncovered and this was used as the starting point of the dataset. Once the stopping condition had been reached, initially a predetermined amount of time, but later changed to a predetermined change in mirror position, then the data acquisition would be stopped in the case of earlier tests, or the detector would be re-covered and then data acquisition would be stopped in later tests.

Analysis of data from earlier tests using the Michelson interferometer did not involve using the Fourier transform; instead interferograms were generated and observed to look for indications of errors in the experimental setup. Observation of these interferograms suggested that the period of oscillation of the intensity, which should have been constant, was varying in time. Further analysis of individual period lengths yielded the interesting but undesirable result that there was a periodicity to these changes in the oscillation. This indicated that there was likely a physical effect on the system that was causing the phenomenon, rather than it being a result of normal random errors in the experiment. Figure 3.4 shows a portion of the scatter plot of the period length of each individual period for one of the scans, with a trend line added for clarity. An oscillating pattern is visible, as described.

Figure 3.4 - Period Variation

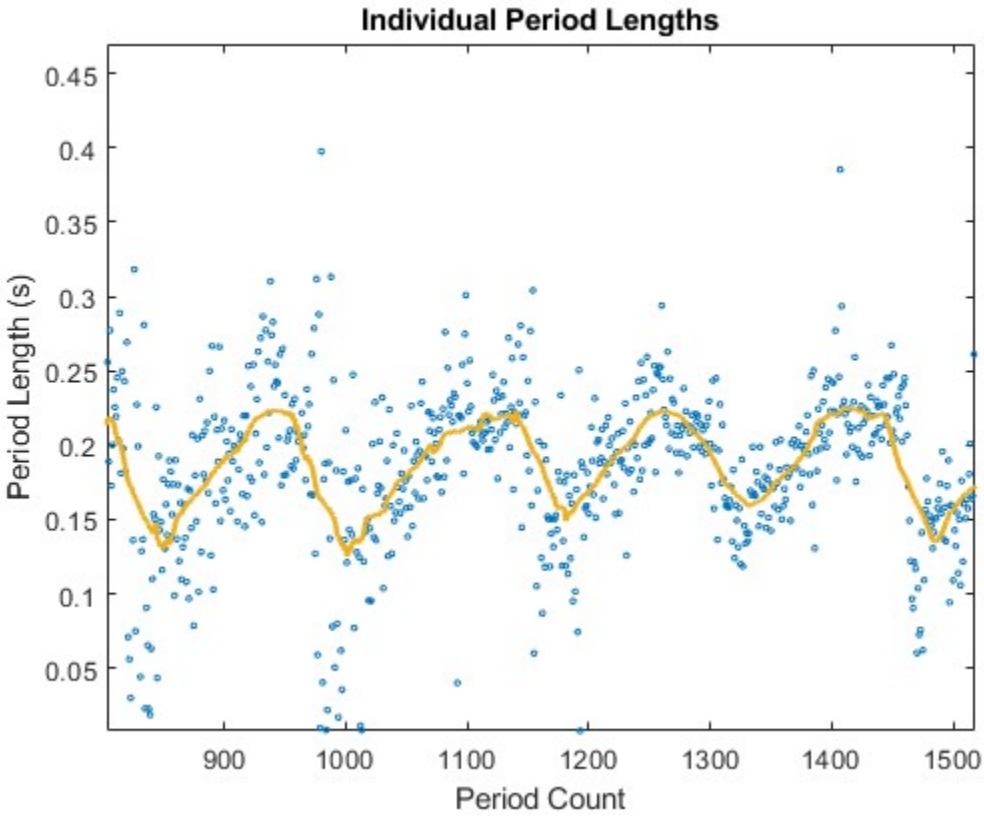

Graph showing variation in length of individual periods across a scan, with trend line added in yellow.

Multiple methods were pursued for the purpose of trying to mitigate this effect as much as possible. An R/C time constant was added to the output from the detector to eliminate high-frequency noise in the signal and produce smoother curves in the datasets. Cushioning was added to the bottom of the board on which the interferometer rested in an attempt to reduce coupling in of any mechanical vibrations present in the building. A transparent plastic cap was placed over the experimental setup to block out small air currents that could cause slight refraction of the light or minutely adjust the positioning or angle of the mirrors. After all of these fixes had been implemented, data were gathered again to determine whether the effect had been eliminated. It was still present, but seemed to be less prominent, so the experiment proceeded.

The first source that was used was a red Helium Neon (HeNe) laser, with a wavelength of 633 nm. In addition to the HeNe laser, other sources were used. Part of the reason for this was to check whether some defect within the laser was affecting the data, though that seemed unlikely. A red diode laser with a variable wavelength was used as a source briefly, though it demonstrated instability in its modes. The laser would randomly switch between resonances, changing its wavelength and making it impossible to take get clean interferograms. It was determined that this source would not be useful.

At this point spectra began to be produced using the FFT. Interferogram data were collected in time, and scan distances were recorded. The total time of a scan was determined from the time data, and the scan length was divided by this number to determine the average translation speed of the mirror. This speed was used to translate the time interferogram into an interferogram for scan distance, assuming constant translation speed throughout the scan, and this distance interferogram was input into the FFT function to generate a spectrum. Figure 3.5 shows a flowchart of this process.

Figure 3.5 – MATLAB Program Flowchart

Flowchart showing process used to create spectra in MATLAB program.

The expectation was to see peaks close to the known emission wavelengths of the various sources, with the rest of the spectrum likely containing some much smaller peaks due to background light in the room and other sources of noise. However, the spectra obtained were not consistent with this expectation. Many of them appeared to have essentially pure noise, with either no peaks rising significantly above the surrounding wavelengths, or slightly elevated points only in areas far away from the wavelength of the laser. A few tests on this and other sources exhibited slight protrusions in the vicinity of the expected wavelengths, but in all of these cases the peaks were not nearly pronounced enough to definitively be a result of the light emitted from the source.

The next source used was a sodium lamp. This source was much dimmer than the lasers, but increasing the sensitivity of the detector and using lenses to focus more of the light into the interferometer allowed it to be usable. Changes in the contrast between the light and dark interference fringes could be observed as the movable mirror changed positions, resulting from beating between the two wavelengths of the sodium doublet. The sodium emission spectrum has one line at 589.0 nm and one at 589.6 nm, with the shorter wavelength being emitted at roughly twice the intensity of the longer one. The slight difference in the oscillation period between these two wavelengths means that when they are superimposed, they oscillate periodically between constructive and destructive interference, resulting in a variation in the amplitude of the combined waveform; a phenomenon known as beating. By taking a long enough interferogram, a full beat period could be recorded, its length could be measured, and the distance between the two sodium emission lines could be calculated. This calculation was done using one of the interferograms (shown in Figure 3.6), and the agreement was reasonably good. This seemed as though it could be a useful and informative addition to the student lab module. However, when the interferograms were put through the FFT, the aforementioned issue occurred, with the spectra being largely nothing but noise (shown in Figure 3.7).

Figure 3.6 - Na Lamp Beat Pattern

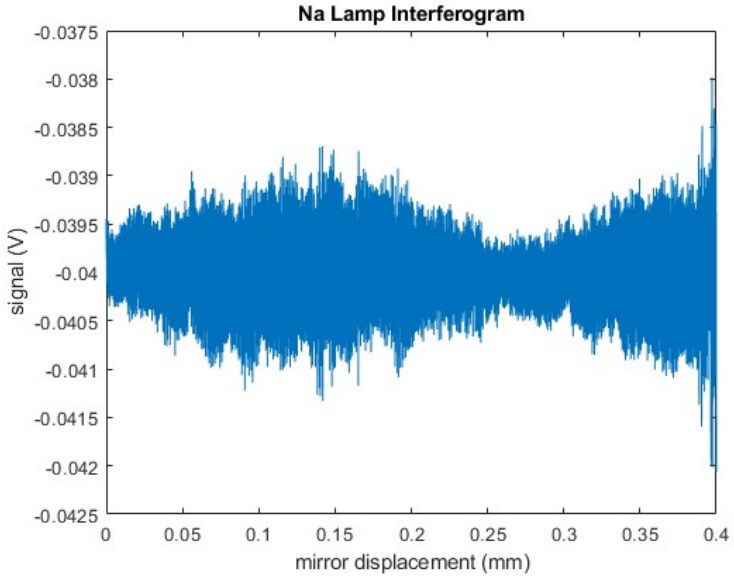

An interferogram collected using the sodium lamp, with a full beat period visible.

Figure 3.7 - Generated Na Lamp Spectrum

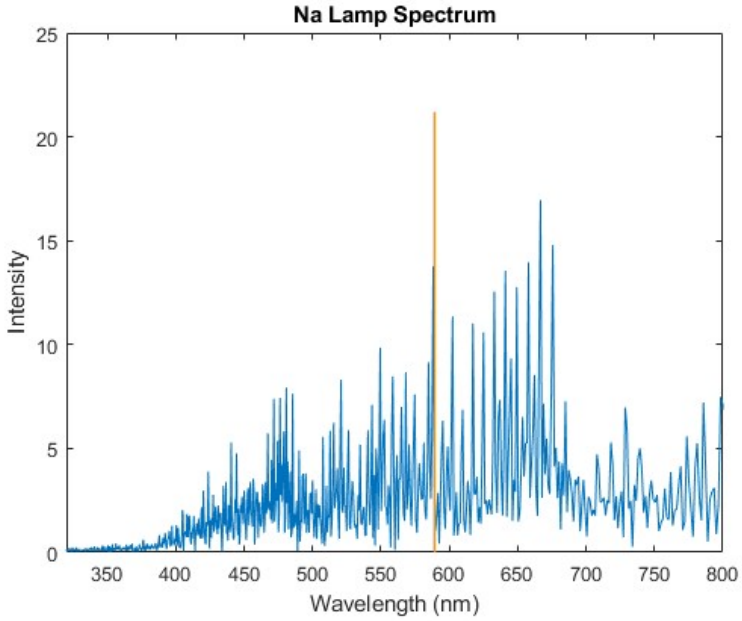

a) The orange line (actually two very close together) shows the wavelengths of the sodium emission lines.

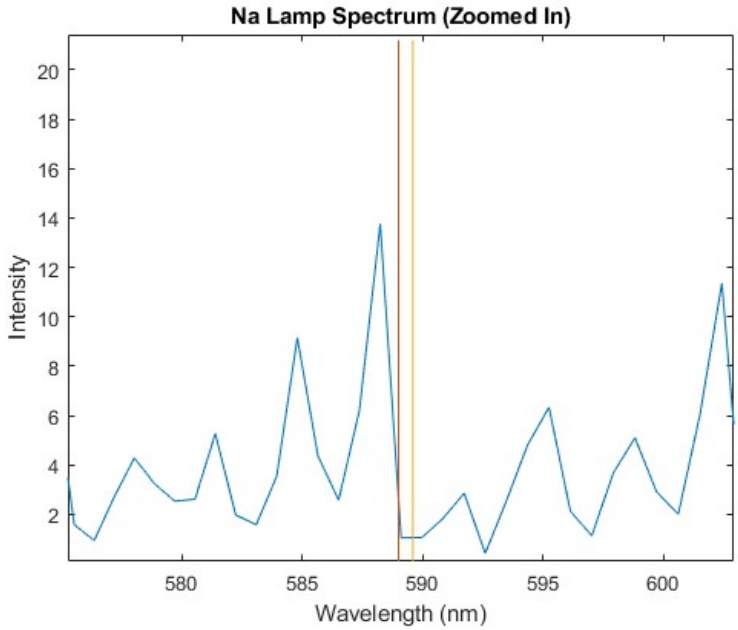

b) A zoomed in view of the region around the actual sodium emission lines.

A mercury lamp was also available, and was used as a source after the sodium lamp. The greater number and wider spread of the mercury emission lines as compared to sodium meant that this source

was not as useful for numerical calculations using the beat pattern. Additionally, this more complex emission spectrum prevents alternate methods of obtaining information about the spectrum such as the counting of periods used on the red HeNe laser (discussed later in this section); the only way is to generate the full spectrum using the interferogram. Unsurprisingly, the spectra generated from the Hg lamp were just as useless as those for the sodium lamp.

Figure 3.8 - Generated Hg Lamp Spectrum

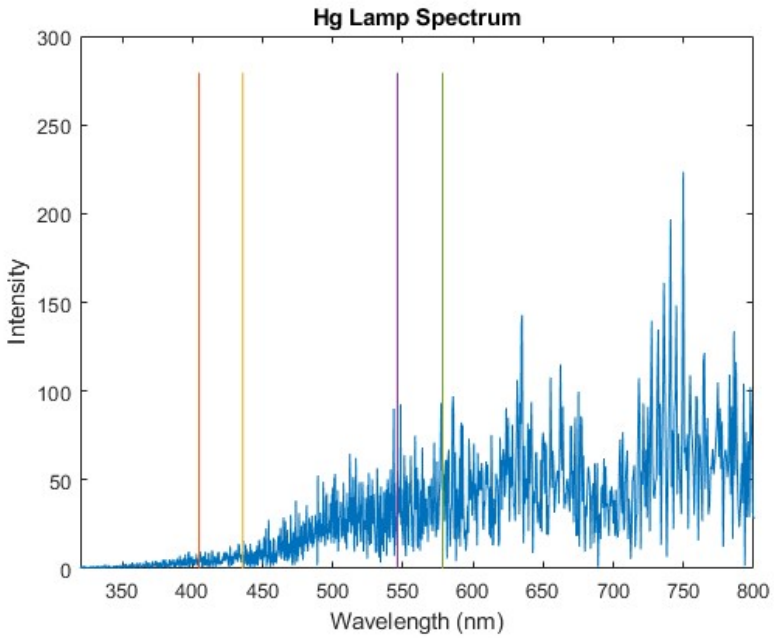

The lines show the actual locations of the mercury emission lines.

Later, it was discovered that in some datasets, some data points would be recorded incorrectly. There were some time values that should have been recorded that were skipped entirely, and others that were recorded twice. This interfered with the ability to properly analyze data and obtain spectra, since the data were recorded using time values, but distance values for the position of the movable mirror were required as inputs for the FFT. This meant that a conversion from time to distance was necessary, requiring that the mirror move at constant speed and requiring that the time steps between each individual data point be consistent, so that the corresponding distance value could be obtained for each data point's time value. With these skips and duplicate points present in the dataset, conversion could not be done properly, so generation of correct spectra was impossible. After this discovery, efforts were made to discover the source of the errors in data recording so that this problem could be eliminated. Eventually, it was determined that the best course of action was to stop using the software, and change the data collection device from the computer to an oscilloscope available in the laboratory.

In the meantime, the wavelength of the red HeNe laser was measured through other means. The mirror was scanned through pre-set distances using the motor, as before, but instead of using

software to record a complete interferogram, a much simpler device was used, which incremented a counter each time two zero crossings (indicative of one period) were detected. Dividing the total change in the mirror path difference, which was twice the change in the position of the movable mirror, by the number of periods the interference pattern went through over that distance, would provide a measurement for the wavelength of the light from the laser.

$$wavelength = \frac{2 * scan\ distance}{number\ of\ periods} \tag{3.1}$$

The actual wavelength of the laser was 633 nm. Here is a table of experimental values from these tests:

Table 3.1 - Calculated Wavelengths of Red HeNe Laser

Mirror Scan Distance (mm)	Number of Periods	Calculated Wavelength (nm)
0.1	271	738.0
0.2	628	636.9
0.1	282	709.2
0.1	306	653.6
0.2	604	662.3
0.2	631	633.9
0.2	558	716.8
0.2	630	634.9
0.2	632	632.9
0.2	629	635.9
0.2	630	634.9
Average		662.7
Standard Deviation		39.4

Data taken by counting periods while scanning using the motor.

One notable feature of the dataset shown in Table 3.1 is the fact that every single one of these measurements is above the expected value of 633 nm, except for 632.9 nm, which is only very slightly below it. This is highly unusual; for a normal dataset it would be expected that even if the mean value of the dataset was not exactly equal to the true value, there should be data points both above and below the true value, since random errors would push the measurement up or down from the true value with equal probability. The fact that these values were so consistently above the true value suggested the presence of some systematic error. The source of that error would be investigated further using the oscilloscope.

Once the oscilloscope began being used, it was confirmed that there were no longer any issues with missing or duplicate data points. However, the issue of being unable to generate spectra which matched the known spectra of the various sources persisted. With the failure to obtain actual spectra

for any of the sources, it was clear that some systematic error was occurring in the apparatus. Appearance of periodic abnormalities in many of the interferograms across different sources seemed to suggest that the error may have been occurring in the mechanism that drove the movable mirror; somewhere in the micrometer, the motor, or the connection between them. Testing showed that the period of these abnormalities synchronized with the period of rotation of the motor, essentially confirming this suspicion. After this, the hardware was scrutinized to find the source of the problems. The final conclusion was that the axle connected to the motor was not firmly attached, and the wobbling of this loose axle during scanning of the motor caused the speed to vary, and sometimes briefly lost connection with the micrometer, resulting in the periodic anomalies. Some attempts were made to tighten this connection, but these were unsuccessful. The final decision was to stop using the motor and simplify the lab to activities that could be done by turning the micrometer by hand.

3.3 Final Refinement of Lab Module

The final sessions in the laboratory were spent ensuring that all procedures planned for use in the lab module were not only able to be done, but able to be done quickly enough to fit into the limited time available in a class setting.

The first procedure to be tested was measurement of the wavelength by counting periods over a known scan length. As discussed in the previous section, this had been done before with the red HeNe laser, but the results were skewed by the defective motor. This time, the motor was not used, with the knob of the differential micrometer instead being turned by hand. Additionally, a newly introduced source was used; a green HeNe laser, with a wavelength of 543.5 nm. Table 3.2 contains one of the datasets collected in this manner.

Table 3.2 - Calculated Wavelengths of Green HeNe Laser

Mirror Scan Distance (mm)	Number of Periods	Calculated Wavelength (nm)
0.05	186	537.6
0.05	184	543.5
0.05	180	555.6
0.05	185	540.5
0.05	183	546.4
Average		544.7
Standard Deviation		6.88

Data taken by counting periods while scanning by turning the micrometer knob by hand.

Data in Table 3.2 were collected using a scan length of 0.05 mm, corresponding to one full rotation of the micrometer knob. It is important to note that this dataset contains measurements that are above and below the true wavelength of 543.5 nm in roughly equal proportion, unlike the earlier

dataset where the motor was used. As a result of this, the average value of the measurements is much closer to the true value. The standard deviation is smaller as well, but that is likely due mostly to better placement of the waveform relative to the zero point, preventing outliers caused by missing periods in some counts, rather than being caused by any effect of removing the motor.

After it was confirmed that removing the motor allowed accurate datasets to be taken, the Na lamp was used again, and this method was applied to attempt to measure the middle wavelength of its doublet structure. The idea was that since the two sodium lines are so close in wavelength, they should generate an interferogram with a base frequency very close to that of a single-wavelength source in the middle of the two. The same method of counting periods was applied, and the agreement between the results and the actual sodium wavelengths was quite good. Here is an example calculation using collected data and Equation (3.1):

$$wavelength = \frac{2 * 0.05\ mm}{170} = 5.882 * 10^{-4}\ mm = 588.2\ nm$$

This is close to the actual middle wavelength of 589.3 nm. Other measurements were similarly close to the actual value.

The next, and final, step was to investigate the one numerical method that showed promise during the main experimental phase: calculating the spacing between the sodium lines using the beat period. This spacing is quite small, about 0.6 nm at a wavelength of about 589 nm, so the period of the beats resulting from this difference is relatively large. Partially because of this, determining a method of measuring the beat spacing while moving the micrometer by hand was a challenge. The first attempted method involved watching the interference pattern directly on a white card and observing at what distance readings the contrast reached two consecutive maxima. It was found to be too difficult to determine when the contrast reached a maximum, and no measurements for the beat period could be obtained. The next method used the oscilloscope, attempting to watch and see when the amplitude reached a minimum. However, turning the knob by hand resulted in choppy movement, and it was impossible to correlate points in the displayed waveform with micrometer readings. After this point, time restraints prevented further investigation, so the results of this segment of the research were inconclusive.

4. Discussion

4.1 Limitations of Apparatus

The eventual simplification of the original vision for the student module was largely due to the limitations of the equipment available for testing. The faulty data acquisition program, though mentioned only briefly, was actually used for a fairly large portion of the testing time. Many datasets were taken using this program, often being unable to produce spectra at all as a result of the defect. The program in question was not originally designed for this application, so that may explain why the issues occurred.

However, even if the datasets had been collected without error from the beginning, they would not have generated the expected spectra, because the motor defect would still have been present. The failure of the motor to maintain constant speed through a scan is what caused the issue. This change in the translation speed of the motor caused the interferograms to display changes in the period of oscillation which were not the result of the actual interference, but actually came about because of the motor. Thus when the Fourier transform decomposed the signals, the frequencies resulting from source wavelengths were not prominent, as they should have been. If the motor had worked properly and translated the mirror at a constant rate, then these frequencies would not have been obscured, and the generated spectra may have been more conclusive.

This is not guaranteed, however, since it is possible that there were other sources of systematic error in the apparatus that went unnoticed as a result of their effects being obscured by the presence of the motor defect. Testing for such sources of error would have required a properly working replacement motor, which was not available.

4.2 Student Module

The final student lab module developed during this project is divided into three sessions, each focusing on a different light source.

4.2.1 Session 1: Red HeNe Laser

Students will begin the first session by practicing aligning the mirrors on the Michelson interferometer. It is very important for these mirrors to be angled correctly in order for an interference pattern to appear. The full process of aligning both mirrors is time-consuming, so the interferometer will be pre-aligned by the lab instructor, then one of the mirrors will be moved out of alignment. The students will be told which mirror needs to be adjusted, and will change the angle of that mirror until the interference pattern becomes clearly visible. This exercise will demonstrate to the students how important it is for the interferometer to be aligned properly.

After the alignment is done, the students will collect data. The procedure will be the same as that used during the final stage of this project's experimental phase. Students will rotate the knob on the differential micrometer one full revolution, and count the number of periods in the interference pattern over that displacement using the provided equipment. This process will be repeated five times, and they will then calculate the mean and standard deviation of their dataset. The students will be asked to do this three times.

They will then be asked to find the true wavelength of the laser using another device, and compare their results to this value.

4.2.2 Session 2: Green HeNe Laser

This session will use the green HeNe laser in order to show students that this method of measuring wavelength can be used at different places on the spectrum, and is not specific to the red light used in Session 1.

The main focus of this session is on data analysis, so the students will be collecting more datasets than in Session 1. They will, as before, collect three datasets with a scan length of one full rotation of the micrometer knob, and they will then be asked to collect three sets each with scan lengths of one-half rotation of the knob and two full rotations of the knob. Students will be asked to observe and comment on differences in the standard deviation of the datasets at different scan lengths. Theoretically, the standard deviation should be smaller for longer scans, since more data, in this case more periods included in the count, results in noise being averaged out, so measurements should generally be closer to the mean.

Students will then be asked to once again verify their results by measuring the wavelength of the laser using another device.

4.2.3 Session 3: Na Lamp

The final session will utilize the sodium lamp. First, students will be asked to rotate the micrometer knob and observe the interference pattern on a surface where it will be clearly visible, such as a white index card. Along with this, and explanation of the theory behind beating will be provided. Numerical calculations of line spacing based on beat period would have been included, since they were successful during experimentation, but no method of measuring the beat period without using the motor could be found.

After this, the same data collection process as in Session 1 will be used. Despite the fact that the sodium emission spectrum contains two wavelengths, rather than one, the fact that they are so close together creates a base oscillation in the interferogram that is very similar to the oscillation that would occur if a single-wavelength source with a wavelength at the average of the two were to be measured. This means that the students can find the average wavelength of the two sodium emission lines.

Finally, they will be asked to confirm their measurements as before.

5. Conclusion

Fourier transform spectroscopy is often a difficult concept to express clearly to students, and there is often a tendency to misunderstand what exactly is being measured and what is merely incidental. Further, interferometry is a crucial component of modern physics and affords extensive practical application in many fields. Exposure to spectroscopy and optical testing is essential for a student

interested light interaction, and as such, these skills are quite valuable. These ambiguities created an opening for our project to provide a beneficial experience to students, and largely served as motivation for our module. The primary limitation of our project was the error in the interferogram due to the irregular periodicity of the synchronous motor, which created complications in regards to the Fourier transform. This however, appears to us as a relative potentiality, and is in no way fatal to the original project vision. By tracing the theoretical principles of FTS alongside our data collection, we put the project in a position to interpret a pathway forward. One of the ways we can envisage a solution would be an alternative drive for the interferometer translation stage. This could be done via a synchronous motor with a constant periodicity, which would improve the quality of the interferogram, and thus, the quality of the returned spectrum. Meanwhile, with this change, new analysis could pick up where this study left off, and return to signal processing.

References

1.) Smith, Brian C. *Fundamentals of Fourier Transform Infrared Spectroscopy*. CRC Press, 2011.
2.) Goodwin, Eric P., and James C. Wyant. *Field Guide to Interferometric Optical Testing*. SPIE Press, 2006.
3.) Bracewell, Ronald N. *The Fourier Transform and Its Applications*. McGraw-Hill.
4.) Hariharan, P. *Basics of Interferometry*. Elsevier Academic Press, 2007.
5.) *Ben Crowell's Physics 221-223 Course at Fullerton College*, www.lightandmatter.com/area3phys221.html.